Pergamon

Chemical Engineering Science, Vol. 49, No. 6, pp. 863–876, 1994

0009-2509/94 $6.00 + 0.00

SIGNIFICANCE OF THE RADIAL POROSITY PROFILE FOR THE DESCRIPTION OF HEAT TRANSPORT IN WALL-COOLED PACKED BEDS

J. G. H. BORKINK and K. R. WESTERTERP†
Chemical Reaction Engineering Laboratories, Department of Chemical Engineering, Twente University of Technology, PO Box 217, 7500 AE Enschede, The Netherlands

(*Received* 19 *November* 1992; *accepted for publication* 23 *July* 1993)

Abstract—The influence of a radial porosity and velocity profile on the predicted temperature and concentration profiles in wall-cooled packed beds is studied, with and without an exothermic first-order chemical reaction, on the basis of literature correlations for the effective transport coefficients. Furthermore, values for the effective heat transport coefficients are obtained from "cold-flow" experiments by means of model fitting, with and without taking the radial velocity profile into account. The radial porosity and velocity profiles are approximated by a step-function, which is referred to as the "two-region model". It is shown that the effective radial heat conductivity can be taken constant over the radius, despite the wall effect. Nevertheless, the influence of a radial superficial velocity profile can be significant through the convective term in the heat balance, especially for low tube-to-particle diameter ratios. The predicted NTU can increase the order of 20% for high values of the Reynolds number and up to 100% for low values. This is confirmed by the results obtained from the model fitting. In case of a first-order exothermic reaction, significantly higher values for the hot-spot temperatures are predicted, if a radial porosity and velocity profile is incorporated in the heat and mass balances. This is found to be mainly caused by the non-uniform distribution of active catalyst over the radius, due to the porosity profile.

INTRODUCTION

Wall-cooled or wall-heated tubular reactors are often used in industry to carry out highly exothermic or endothermic, heterogeneous gas–solid reactions. Until now, it has not been possible to design these reactors on the basis of kinetic experiments, cold-flow experiments and computer calculations alone [see, e.g., Paterson and Carberry (1983), Eigenberger and Ruppel (1985) and Feyo de Azevedo *et al.* (1990)]. The available mathematical models are not believed to be reliable enough, nor the experimental data for the parameter values to be used. A large spread is observed in the experimental values for the heat transport coefficients as presented by different investigators [see, e.g., Li and Finlayson (1977), Ziolkowski and Legawiec (1987), Gunn *et al.* (1987), Tsotsas and Schlunder (1990) and Freiwald and Paterson (1992)], which may be caused by a lack of consistency between the different models and/or experimental apparatus used. When deriving a mathematical model, assumptions have to be made. If one or more of these are invalid, the model predictions become reference-frame-dependent. An assumption often made is that of a constant porosity and therefore constant velocity over a cross section in a packed bed. Here, the influence of this assumption on the model predictions is looked at in more detail.

Recently, several investigators have studied the influence of the so called "wall channelling" of the gas on the performance of a cooled tubular reactor [see, e.g., Lerou and Froment (1977), Kalthoff and Vortmeyer (1980), Eigenberger and Ruppel (1985), McGreavy and Foumeny (1986), McGreavy *et al.* (1986), Vortmeyer (1988), Delmas and Froment (1988), Gatica *et al.* (1989) and Vortmeyer and Haidegger (1991)]. Usually this is done by numerically solving the momentum balance together with the heat and mass balances for the packed bed. A large influence of the inclusion of this radial velocity profile on the calculated temperature profiles is often claimed, especially with highly exothermic reactions. However, from literature it is not clear what phenomenon really causes the observed influence. Is it the presence of a radial superficial velocity profile, the radial distribution of active catalyst, or is it the radial variation of the effective heat transport coefficients? Furthermore, it is not clear whether there is any influence to be expected, from the inclusion of a radial velocity profile, on the experimental values for the effective heat transport coefficients, as obtained from packed bed experiments without a chemical reaction.

In this investigation we will show that the presence of a radial superficial velocity profile influences the calculated rate of heat transport for a packed bed through the axial convection term in the heat balance. We will give several arguments, including experimental, for taking the effective radial heat conductivity as being constant over the radius. Furthermore, we will show the influence of the inclusion of a radial porosity and velocity profile with an exothermic reaction, to be mainly caused by the assumption of a radial distribution of active catalyst.

THEORETICAL BACKGROUND

If heat, in a wall-cooled packed bed without reaction, is transported radially by a dispersion mechanism, and if the gas velocity and heat transport

†Author to whom correspondence should be addressed.

parameters are constant over the radius, the radial temperature profile has a parabolic shape. However, Froment and co-workers (1972, 1977) presented experimental radial temperature profiles with several regions near the wall of the tube, in which a flattening of the radial temperature profile occurs. This was attributed to a higher local gas velocity, referred to as "wall channelling" of the gas, supposedly leading to higher values of the heat transport coefficients. In order to qualitatively study the influence of this phenomenon on the model predictions for wall-cooled packed beds, with and without reaction, we use a simple model. The packed bed is divided into two regions, each with a different but constant porosity and superficial velocity, and with its own value for the effective radial heat conductivity [see also Martin (1978) and Tsotsas and Schlunder (1988)]. Furthermore, a wall heat transfer coefficient is assumed at the wall. This is a simplified version of the "wall heat transfer (WHT) model" as presented by Vortmeyer and Haidegger (1991). The step functions for the porosity and velocity are shown in Fig. 1. The porosities and superficial velocities in the core- and wall-region and the width of the wall-region are calculated from the radial profiles as given by Vortmeyer and Schuster (1983). This is shown in Appendices A and B. With these simplifications it is possible to solve analytically the heat balance for a wall-cooled packed bed without chemical reaction, using the Laplace-transform and complex inversion formula. We refer to this as the two-region model, which is not to be confused with the models introduced by Botterill and Denloye (1978), McGreavy *et al.* (1986) and Gunn *et al.* (1987). They also consider a wall and a core region, but in their models the wall region is small and used to describe the sharp decrease in effective radial heat conductivity close to the wall, which is an alternative to using a wall heat transfer coefficient.

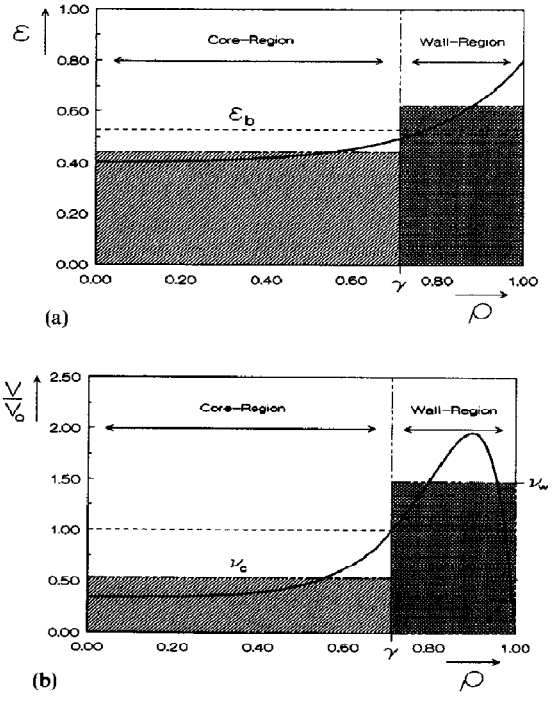

Fig. 1. The porosity and velocity profiles and their approximations in a two-region model, (- - - -) indicating the averaged value. (A) Porosity profile, (B) velocity profile.

The two-region model without a chemical reaction

The influence of a wall effect, as depicted in Fig. 1, on the predicted temperature profile, is first studied for a hot gas that is cooled down in a wall-cooled packed tube, without reaction. For this system the following assumptions are made: —the system is in steady state, —the system is considered to be pseudo-homogeneous, —there is no axial dispersion of heat, —there is no free convection of heat, —there is no radiation, —the pressure is constant in the packed bed, —the wall temperature is constant and —the physical properties of the gas and solid are independent of temperature. With plug flow for the gas, the well known pseudo-homogeneous two-dimensional *one-region model* holds:

$$\frac{\partial\theta}{\partial\omega} = \frac{1}{Bo^{\ominus}_{h,r}}\frac{1}{\rho}\frac{\partial}{\partial\rho}\left[\rho\frac{\partial\theta}{\partial\rho}\right] \tag{1}$$

subject to

$$\omega = 0, \quad \text{all } \rho, \ \theta = 1 \tag{2a}$$

$$\rho = 0, \quad \text{all } \omega, \ 0 \leqslant \theta \leqslant 1 \tag{2b}$$

$$\rho = 1, \quad \text{all } \omega, \ \frac{\partial\theta}{\partial\rho} = -Bi_t\theta \tag{2c}$$

and with the solution

$$\theta(\rho,\omega) = 2\sum_{i=1}^{\infty}\left\{\frac{[J_1(\beta_i)J_0(\beta_i\rho)]}{\beta_i[J_0^2(\beta_i)+J_1^2(\beta_i)]}\exp\left[\frac{-\beta_i^2\omega}{Bo^{\ominus}_{h,r}}\right]\right\} \tag{3a}$$

in which β_i is found from

$$\beta_i J_1(\beta_i) - Bi_t J_0(\beta_i) = 0. \tag{3b}$$

See the notation for the significance of the symbols used. From eq. (3) it follows that the temperature in a wall-cooled packed bed is described by two model parameters $Bo^{\ominus}_{h,r}$ and Bi_t, which contain two heat transfer properties, the effective radial heat conductivity $\lambda_{e,r}$ and the wall heat transfer coefficient α_w. In literature it is sometimes argued that the use of the latter coefficient should be avoided, because it has no physical meaning for low gas velocities [see Tsotsas and Schlunder (1990)]. But, due to the fact that in our modelling the effective radial heat conductivity is taken constant in the wall region, we need this wall heat transfer coefficient to account for the increased heat transfer resistance very close to the wall.

In case the velocity profile is approximated by two different velocities, the following *two-region model* is

obtained:

$$0 \leqslant \rho \leqslant \gamma, \quad \frac{\partial \theta_c}{\partial \omega} = \frac{1}{Bo^{c\Theta}_{h,r}} \frac{1}{\rho} \frac{\partial}{\partial \rho}\left[\rho \frac{\partial \theta_c}{\partial \rho}\right] \tag{4a}$$

$$\gamma < \rho \leqslant 1, \quad \frac{\partial \theta_w}{\partial \omega} = \frac{1}{Bo^{w\Theta}_{h,r}} \frac{1}{\rho} \frac{\partial}{\partial \rho}\left[\rho \frac{\partial \theta_w}{\partial \rho}\right]. \tag{4b}$$

The indices c and w refer to the core and the wall region of the packed bed, respectively. The boundary conditions are:

$$\omega = 0, \quad \text{all } \rho, \ \theta_c = \theta_w = 1 \tag{5a}$$

$$\rho = 0, \quad \text{all } \omega, \ 0 \leqslant \theta_c, \ \theta_w \leqslant 1 \tag{5b}$$

$$\rho = \gamma, \quad \text{all } \omega, \ \theta_c = \theta_w \tag{5c}$$

$$\rho = \gamma, \quad \text{all } \omega, \ \frac{\partial \theta_w}{\partial \rho} = \eta_h \frac{\partial \theta_c}{\partial \rho} \tag{5d}$$

$$\rho = 1, \quad \text{all } \omega, \ \frac{\partial \theta_w}{\partial \rho} = -Bi_t \theta_w \tag{5e}$$

and where γ is the width of the core region and η_h is the quotient of the effective radial heat conductivities in the core region and the wall region. Solving this set of equations yields

$$\theta_c = -\frac{4}{\pi\gamma} \sum_{i=1}^{\infty} \left\{ \frac{J_0(\mu\beta_i\rho)}{\beta_i^2 \Omega(\beta_i)} \exp\left[\frac{-\beta_i^2 \omega}{Bo^{w\Theta}_{h,r}}\right] \right\} \tag{6a}$$

$$\theta_w = -2 \sum_{i=1}^{\infty} \left\{ \frac{[J_0(\mu\beta_i\rho) Q_0(\beta_i\rho,\gamma\beta_i) + \eta_h \mu J_1(\mu\beta_i\rho) P_0(\beta_i\rho,\gamma\beta_i)]}{\beta_i^2 \Omega(\beta_i)} \exp\left[\frac{-\beta_i^2 \omega}{Bo^{w\Theta}_{h,r}}\right] \right\} \tag{6b}$$

in which β_i is found from

$$J_0(\mu\gamma\beta_i)\left\{Q_0(\beta_i,\gamma\beta_i) + \frac{\beta_i}{Bi_t} P_1(\beta_i,\gamma\beta_i)\right\} + \eta_h \mu J_1(\mu\gamma\beta_i)\left\{P_0(\beta_i,\gamma\beta_i) - \frac{\beta_i}{Bi_t} Q_0(\gamma\beta_i,\beta_i)\right\} = 0 \tag{6c}$$

and where

$$\Omega(\beta_i) = J_0(\mu\gamma\beta_i)\left\{ -\left(\frac{1}{\beta_i} + \frac{\beta_i}{Bi_t}\right) Q_0(\beta_i,\gamma\beta_i) + \frac{\gamma\beta_i}{Bi_t}(1-\eta_h\mu^2) Q_0(\gamma\beta_i,\beta_i) + \gamma(\eta_h\mu^2 - 1) + \eta_h\mu\left(\frac{1}{Bi_t} - 1\right) Q_0(\gamma\beta_i,\beta_i) - \eta_h\mu\left(\frac{1}{\beta_i} + \frac{\beta_i}{Bi_t}\right) \times P_0(\beta_i,\gamma\beta_i) + \frac{\mu\gamma\beta_i}{Bi_t}(\eta_h - 1) P_1(\beta_i,\gamma\beta_i)\right\}. \tag{6d}$$

In these equations J_0 and J_1 are Bessel functions of the first kind and Q_0, P_0 and P_1 are cross-products of Bessel functions [see Abramowitz and Stegun (1972) and the notation], and, further, $\mu = \sqrt{(Bo^{c\Theta}_{h,r}/Bo^{w\Theta}_{h,r})}$. For the two-region model, the temperature profile in a wall-cooled packed bed is described by five model parameters: $Bo^{c\Theta}_{h,r}$, $Bo^{w\Theta}_{h,r}$, Bi_t, γ and η_h. If the velocity profile is known, γ can be calculated and only η_h, $Bo^{c\Theta}_{h,r}$, $Bo^{w\Theta}_{h,r}$ and Bi_t remain, containing the three heat transport coefficients $\lambda^c_{e,r}$, $\lambda^w_{e,r}$ and α_w.

The influence of the presence of a radial velocity profile on the performance of a wall-cooled tube, can be judged by comparing the number of heat transfer units NTU for the two models. This number can be calculated according to

$$NTU = -\ln\{\langle\theta\rangle|_{\omega=1}\} \tag{7}$$

in which $\langle\theta\rangle|_{\omega=1}$ is the so called "mean-cup" averaged temperature at the exit of the packed bed, given by

$$\langle\theta\rangle|_{\omega=1} = 2\int_0^1 \rho v \theta|_{\omega=1} \, d\rho. \tag{8}$$

For the one-region model, eq. (8) together with eq. (3) yields

$$\langle\theta\rangle|_{\omega=1} = 4 \sum_{i=1}^{\infty} \left\{ \frac{J_1^2(\beta_i)}{\beta_i^2 [J_0^2(\beta_i) + J_1^2(\beta_i)]} \exp\left[\frac{-\beta_i^2}{Bo^{\Theta}_{h,r}}\right] \right\} \tag{9}$$

in which β_i is found from eq. (3b). For the two-region model, eq. (8) together with eq. (6) yields

$$\langle\theta\rangle|_{\omega=1} = -\frac{8v_c}{\pi\mu} \sum_{i=1}^{\infty} \left\{ \frac{J_1(\mu\gamma\beta_i)}{\beta_i^3 \Omega(\beta_i)} \exp\left[\frac{-\beta_i^2}{Bo^{w\Theta}_{h,r}}\right] \right\} - 4v_w \sum_{i=1}^{\infty} \left\{ \frac{\left[J_0(\mu\gamma\beta_i) P_1(\gamma\beta_i,\beta_i) + \eta_h\mu J_1(\mu\gamma\beta_i)\left\{Q_0(\gamma\beta_i,\beta_i) - \frac{2}{(\pi\beta_i)}\right\}\right]}{\beta_i^2 \Omega(\beta_i)} \exp\left[\frac{-\beta_i^2}{Bo^{w\Theta}_{h,r}}\right] \right\} \tag{10}$$

in which β_i and $\Omega(\beta_i)$ are found from eq. (6c) and (6d), respectively.

Values for the model parameters $Bo^{c\Theta}_{h,r}$, $Bo^{w\Theta}_{h,r}$, Bi_t, γ and η_h can be calculated for given values of the Reynolds number Re^s_p, the number of particles on a diameter N and the tube slenderness Γ. For the

superficial velocity and porosity in the wall- and core-region, the relations proposed by Vortmeyer and Schuster (1983) are used. For the effective radial heat conductivities, $\lambda_{e,r}$, the relation given by Zehner and Schlunder (1970, 1973) is used and for the wall heat transfer coefficient α_w the relation given by Wellauer *et al.* (1982) is used. Because there are no literature relations available for effective heat conductivities in the wall- and core-region separately, we assumed the relation given for a packed bed as a whole can also be used in the two regions individually, using the superficial velocity and porosity for these regions.

The two-region model with a chemical reaction

The influence of the wall effect, as depicted in Fig. 1, on the temperature and conversion profiles, is also studied for an exothermic first-order reaction, $A \rightarrow \nu_p P$, carried out in a cooled tubular reactor with a uniform wall temperature. For this system the same assumptions are made as in the previous section, together with the assumption that the superficial velocity is constant in axial direction, which is in principle only valid for constant density and thus $\nu_p = 1$, see Bos and Westerterp (1990). For the two-region model the following mass and heat balances can be derived for the core region:

$$0 \leqslant \rho \leqslant \gamma,$$

$$\frac{\partial X_c}{\partial \omega} = \frac{1}{Bo^{c\Theta}_{m,r}} \frac{1}{\rho} \frac{\partial}{\partial \rho}\left(\rho \frac{\partial X_c}{\partial \rho}\right) + Da^{\Theta}_c (1 - X_c) \exp\left[\frac{\kappa \Theta_c}{(1 + \Theta_c)}\right] \tag{11a}$$

$$\frac{\partial \Theta_c}{\partial \omega} = \frac{1}{Bo^{c\Theta}_{h,r}} \frac{1}{\rho} \frac{\partial}{\partial \rho}\left(\rho \frac{\partial \Theta_c}{\partial \rho}\right) + Da^{\Theta}_c \Delta T_{ad} (1 - X_c) \exp\left[\frac{\kappa \Theta_c}{(1 + \Theta_c)}\right] \tag{11b}$$

and for the wall region:

$$\gamma < \rho \leqslant 1$$

$$\frac{\partial X_w}{\partial \omega} = \frac{1}{Bo^{w\Theta}_{m,r}} \frac{1}{\rho} \frac{\partial}{\partial \rho}\left(\rho \frac{\partial X_w}{\partial \rho}\right) + Da^{\Theta}_w (1 - X_w) \exp\left[\frac{\kappa \Theta_w}{(1 + \Theta_w)}\right] \tag{12a}$$

$$\frac{\partial \Theta_w}{\partial \omega} = \frac{1}{Bo^{w\Theta}_{h,r}} \frac{1}{\rho} \frac{\partial}{\partial \rho}\left(\rho \frac{\partial \Theta_w}{\partial \rho}\right) + Da^{\Theta}_w \Delta T_{ad} (1 - X_w) \exp\left[\frac{\kappa \Theta_w}{(1 + \Theta_w)}\right] \tag{12b}$$

subject to:

$$\omega = 0, \text{ all } \rho, \quad X_c = X_w = 0 \text{ and } \Theta_c = \Theta_w = 0 \tag{13a}$$

$$\rho = 0, \quad \text{all } \omega, \frac{\partial X_c}{\partial \rho} = 0 \text{ and } \frac{\partial \Theta}{\partial \rho} = 0 \tag{13b}$$

$$\rho = \gamma, \quad \text{all } \omega, \quad X_c = X_w \text{ and } \Theta_c = \Theta_w \tag{13c}$$

$$\rho = \gamma, \quad \text{all } \omega, \quad \frac{\partial X_w}{\partial \rho} = \eta_m \frac{\partial X_c}{\partial \rho} \text{ and } \frac{\partial \Theta_w}{\partial \rho} = \eta_h \frac{\partial \Theta_c}{\partial \rho} \tag{13d}$$

$$\rho = 1, \quad \text{all } \omega, \quad \frac{\partial X_w}{\partial \rho} = 0 \text{ and } \frac{\partial \Theta_w}{\partial \rho} = -Bi_t \Theta_w. \tag{13e}$$

The two Da^{Θ} numbers incorporate both the differences in superficial velocity, as well as the effect of a difference in the amount of catalyst per unit of reactor volume, due to the difference in porosity (see the notation). The two $Bo^{\Theta}_{h,r}$ numbers incorporate both the differences in superficial velocity and the differences in effective radial heat conductivity. By introducing $Bo^{c\Theta}_{m,r} = Bo^{w\Theta}_{m,r}$, $Da^{\Theta}_c = Da^{\Theta}_w$, $\eta_h = 1$ and $\eta_m = 1$ into eqs (11) and (12), the partial differential equations for the *one-region model* are obtained again.

The partial differential equations are non-linear and therefore, cannot be solved analytically. A numerical method is applied, using a fourth-order Runge–Kutta method in the axial direction together with a collocation method in radial direction, see Villadsen and Stewart (1967), with four interior points at 0.394γ, 0.803γ, γ and $\gamma + 0.577(1 - \gamma)$, respectively.

From eqs (11) and (12) it follows that the temperature and conversion profiles can be calculated for known values of $Bo^{c\Theta}_{m,r}$, $Bo^{w\Theta}_{m,r}$, $Bo^{c\Theta}_{h,r}$, $Bo^{w\Theta}_{h,r}$, Da^{Θ}_c, Da^{Θ}_w, Bi_t, γ, η_h and η_m. These model parameters can be determined for given values of Re^{*}_p, N, Γ, κ, Da_0 and ΔT_{ad}, using the relations of Vortmeyer and Schuster (1983), Zehner and Schlunder (1970, 1973) and Wellauer *et al.* (1982) and the relation of Fahien and Smith (1955) for the effective radial mass dispersion coefficient $D_{e,r}$. The one-region model can now be compared to the two-region model on the basis of the calculated temperature in the hot spot.

MODEL FITTING AND EXPERIMENTAL SET-UP

Model fitting to experimental temperature profiles

Besides performing model calculations, based on literature relations for the effective heat transport coefficients, the one- and two-region models without a chemical reaction are also used to obtain experimental values for these coefficients by fitting the model solutions to experimentally obtained temperature profiles. By fitting the *one-region model* to the measured axial and radial temperature profiles, values for the effective radial heat conductivity $\lambda_{e,r}$ and the wall heat transfer coefficient α_w are obtained. But, for the *two-region model*, several possibilities exist to obtain best fit values for the heat transport coefficients. In principle, it is possible to fit all five model parameters simultaneously. However, the shape of the radial temperature profile is not much affected by a radial velocity profile and, thus, it is hardly possible to obtain reliable values for the parameters describing this velocity profile in this way. Therefore, the basic velocity profile has again been taken from Vortmeyer and Schuster (1983). Although they measured velocity profiles for spherical particles only, we used their data

also for non-spherical particles, like cylinders and Raschig rings. This may lead to erroneous parameter values, but still enables us to evaluate the influence of the higher gas velocity in the wall region. Consequently, only the three coefficients $\lambda^c_{e,r}$, $\lambda^w_{e,r}$ and α_w are fitted for the two-region model. If the effective radial heat conductivity is taken constant over the radius, $\lambda^c_{e,r} = \lambda^w_{e,r}$, the two-region model yields only two parameters $\lambda_{e,r}$ and α_w. The model fitting is performed by minimizing a chi-square target function which is given by

$$\chi^2 = \sum_{i=1}^{n} \left(\frac{\theta_i - \theta(\rho,\omega,\lambda_{e,r},\alpha_w)}{\sigma_i} \right)^2. \qquad (14)$$

In eq. (14) n is the number of measured temperatures, θ_i is the experimentally obtained temperature, $\theta(\rho,\omega,\lambda_{e,r},\alpha_w)$ is the value predicted by the one-region or the two-region model and σ_i is the standard deviation for the measured temperatures. The chi-square target function is minimized by using a downhill simplex method in multidimensions with different starting points [see Press *et al.* (1989)].

Experimental set-up

The experimental set-up to measure radial and axial temperature profiles contained three stainless steel wall-cooled tubes, with a length of 1.33 m and inner diameters of 44.9, 63.5 and 99.0 mm, respectively. The tubes were filled with a packing and cooled at the wall with water of about 283 K, flowing through a jacket. Upwards flowing hot air of about 333 K was cooled down in the tubes. The radial temperature profile was measured in the packed bed near the top, with 7–15 K-type thermocouples of 0.5 mm diameter, fixed in a rectangular rod of 2×2 mm, which was placed radially through the centre of the packed bed. The rod consisted of a low-conducting, fibre-reinforced epoxy-resin with $\lambda_s = 0.6$ W/m K, so that the measured temperatures were not influenced by conduction through the rod [see, e.g., Dixon (1988) and Wijngaarden (1988)]. The temperature of the gas at the inlet of the packed bed, the coolant temperature at the inlet and the outlet, the pressure before and after the bed and the gas flow rate were also measured. The bed length in the tubes could be increased by lowering the piston in the bottom of the tubes and adding extra packing material at the top, keeping the top of the packing at the same place in the tube. By changing the bed height in this way it was possible to obtain radial temperature profiles at different axial positions or bed lengths. The tubes were also designed such that the bed could easily be repacked, by fluidizing the packing for a short time. In this way several radial temperature profiles were determined for the same experimental conditions, and these were averaged to one mean profile. Care was taken that the bed height, and thus average bed porosity, was always the same for one experimental series.

All experiments reported here have been performed with air at atmospheric pressure, for which the following physical properties at 1 bar and 313 K were used: $\rho_g = 1.13\ \mathrm{kg\,m^{-3}}$, $Cp_g = 1014\ \mathrm{J\,kg^{-1}\,K^{-1}}$, $\eta_g = 19.04\ 10^{-6}$ Pa s and $\lambda_g = 0.027\ \mathrm{W\,m^{-1}\,K^{-1}}$. The pressure drop over the packed bed was always below 0.1 bar and therefore neglected. Different kinds of packings were used, e.g. glass spheres of $d^e_p = 3.7$ and 7.2 mm, porous alumina cylinders of $d^e_p = 5.9$ mm and porous alumina Raschig rings of $d^e_p = 6.2$ mm. Only the results for the glass spheres will be presented here. The measured average bed porosities ε_b are given in Table 1 for the different tubes and glass spheres used. For a more detailed description of the measuring procedure and packings used, the reader is referred to Borkink (1991) and Borkink and Westerterp (1992).

RESULTS OF THE MODEL CALCULATIONS AND THE MODEL FITTING

Model calculations without a chemical reaction

Several temperature profiles were calculated for the one- and two-region models, using literature relations for the heat transport coefficients on the basis of the superficial velocity. Although, a difference in effective radial heat conductivity between the core and wall region is predicted by the literature relations, there was no significant flattening observed of the radial temperature profile near the wall. In fact, it became impossible to obtain any flattening of the radial temperature profile, when using literature relations for the heat transport coefficients. The ratio of the heat conductivities in the core and the wall region η_h was always between 0.5 and 1.2. Only very small values for η_h, say < 0.2, would lead to some flattening of the radial temperature profile near the tube wall.

Table 1. Measured average bed porosities for the different tubes and packings used for the experiments discussed in this article

		Tubes		
		I $D_t = 49.9$ mm	II $D_t = 63.5$ mm	III $D_t = 99.0$ mm
Glass spheres	A $d^e_p = 3.7$ mm	0.36	X	X
	B $d^e_p = 7.2$ mm	0.39	0.38	0.37

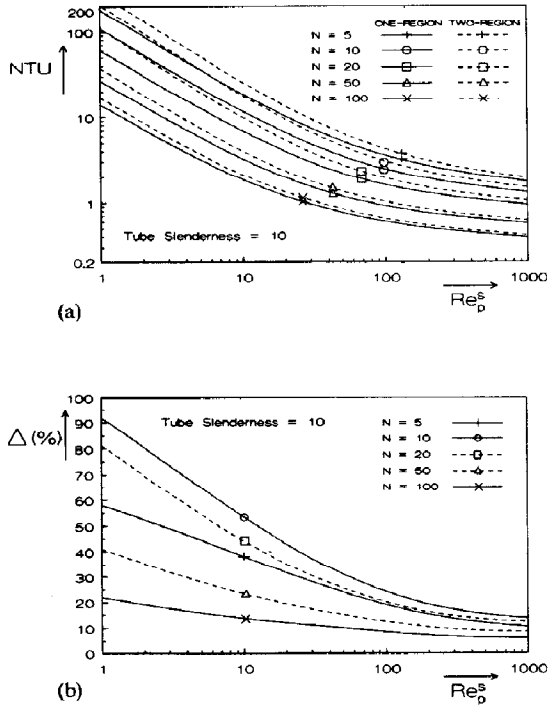

Fig. 2. Calculated values for NTU for laboratory conditions with $\Gamma = 10$ and $\lambda_{e,r}^c = \lambda_{e,r}^w$. (A) NTU vs Re_p, (B) difference vs Re_p. $\Delta = \{(NTU_{\text{two-region}}/NTU_{\text{one-region}}) - 1\}100\%$.

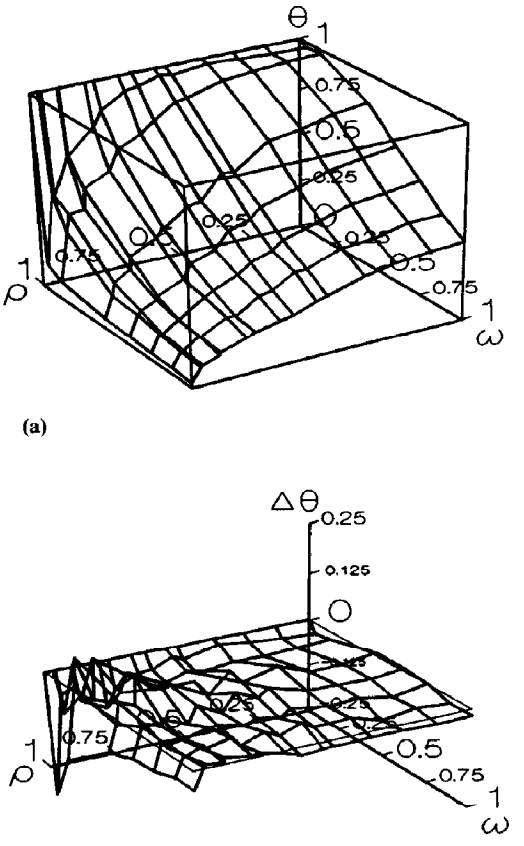

Fig. 3. Experimental and fitted temperature profiles for tube III with $D_t = 99.0$ mm, glass spheres with $d_p^s = 7.2$ mm and $G = 1.13\ \text{kg m}^{-2}\text{s}^{-1}$. $\Delta = \theta_{\text{exp}} - \theta_{\text{cal}}$. (A) Experimental profile, (B) difference plot.

In Fig. 2(a), calculated values of the NTU, for the two models, are given as a function of Re_p^s and for certain values of the number of particles on a diameter N and tube slenderness Γ. It should be noted that the effective radial heat conductivities in the core and the wall region are taken to be the same. The results hardly change if the heat conductivities in the two regions are not taken to be equal. Thus, the difference in NTU for the two models is the result of the difference in superficial velocity in the two regions, and not the result of a difference in heat conductivity. In Fig. 2(b), the differences in NTU for the two models are given. The difference in NTU for $N = 5$ being smaller than that for $N = 10$ and $N = 20$ is due to the behaviour of the predicted velocity profile for low values of N (see Appendix B).

Model fitting without a chemical reaction

The experimental approach led to a vast amount of results, which will now be partly discussed. In Fig. 3(a), an example is shown of an averaged, experimental temperature field. This temperature field is used to determine the heat transport parameters, by fitting the two models to these profiles. In Fig. 3(b), the differences between the measured and best fitting profile are shown. Because, the temperatures measured very close to the wall were probably influenced by conduction to this wall [see Borkink (1991)] they were never used for fitting the models. In Figs 4 and 5, the best fit values for the dimensionless heat transport coefficients are given for the different tube nos I and III and for the glass spheres type A or B (see Table 1) as a function of the Peclet number. Although the type of gas was not changed, a Peclet number is used in accordance with the results of, e.g., Agnew and Potter (1970) and Olbrich and Potter (1972). In Fig. 4, they are given for the one- and two-region model with two parameters $\lambda_{e,r}$ and α_w, respectively and, in Fig. 5, they are also given for the two-region model with three parameters $\lambda_{e,r}^c$, $\lambda_{e,r}^w$ and α_w. The two-region model with different heat conductivities in the core and the wall region has not been applied to tube I with $D_t = 49.9$ mm and tube II with $D_t = 63.5$ mm, because for these tubes only six radial temperatures were available for the fitting. With such a small number of radial temperatures, it was not possible to get realistic values for the effective radial heat conductivity in the wall region and the wall heat transfer coefficient. For tube III with $D_t = 99.0$ mm, the number of available radial temperatures was 14. In the figures, the para-

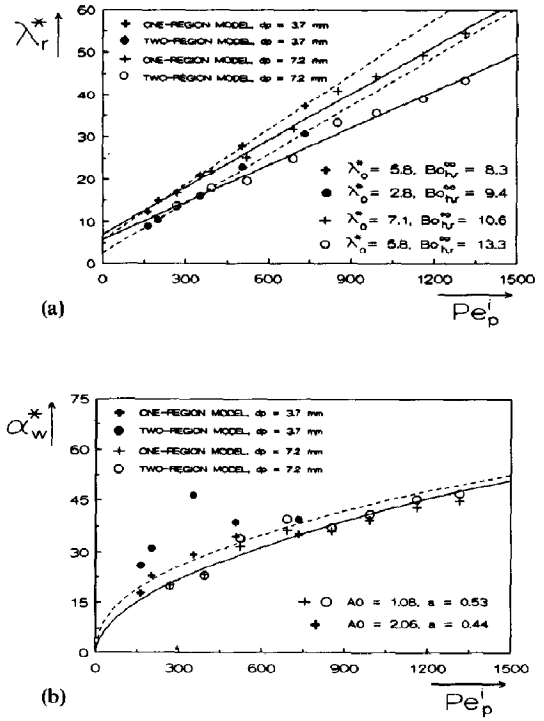

Fig. 4. Values for the effective radial heat conductivity and the wall heat transfer coefficient for tube I with $D_t = 49.9$ mm and glass spheres with $d_p^e = 3.7$ and 7.2 mm. The meaning of λ_0^* and $Bo_{h,r}^\infty$ are given by eqs (15). (A) Effective radial heat conductivity, (B) wall heat transfer coefficient.

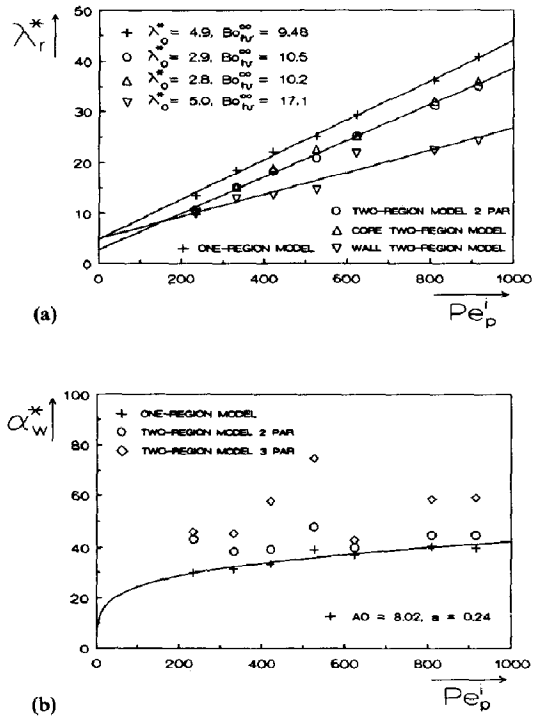

Fig. 5. Values for the effective radial heat conductivity and the wall heat transfer coefficient for tube III with $D_t = 99.0$ mm and glass spheres with $d_p^e = 7.2$ mm. (A) Effective radial heat conductivity, (B) wall heat transfer coefficient.

meters λ_r^* and α_w^* are correlated by

$$\lambda_r^* = \lambda_0^* + \frac{\varepsilon_b Pe_p^i}{Bo_{h,r}^\infty} \quad 100 < Pe_p^i < 1500 \qquad (15)$$

and

$$\alpha_w^* = A0\{Pe_p^i\}^a \quad 100 < Pe_p^i < 1500 \qquad (16)$$

in which $\lambda_r^* = \lambda_{e,r}/\lambda_g$ and $\alpha_w^* = \alpha_w d_p^e/\lambda_g$. The coefficients λ_0^*, $Bo_{h,r}^\infty$, $A0$ and a used in eqs (15) and (16) are given in the figures. $Bo_{h,r}^\infty$ is the Bodenstein number for heat if only radial dispersion takes place.

Because a chi-square fit is used it is possible to calculate the so called "goodness-of-fit" (GOF) [see Press *et al.* (1989)]. This GOF is the probability that the chi-square exceeds a particular value χ^2_{min} by chance. This probability is calculated using the chi-square distribution for $n - m$ degrees of freedom, where n is the number of measured points and m the number of adjustable parameters. If the GOF is a very small probability for some particular data set, then the apparent discrepancies are unlikely to be accidental fluctuations. In this case, either the model is wrong or the measurement errors are really larger than stated. In Table 2, values for the GOF for tube I with $D_t = 49.9$ mm are given for the one-region and two-region model, together with values for the mean error of the fits. This value is calculated according to

$$\text{Error} = \frac{\sum_{i=1}^{n} (\theta_i - \theta(\rho, \omega, \lambda_{e,r}, \alpha_w))}{\sum_{i=1}^{n} \theta_i} 100\%. \qquad (17)$$

Uniform or radially varying effective heat conductivity?

In Fig. 6, a radial superficial velocity profile is given as calculated on the basis of the data of Vortmeyer and Schuster (1983) (see Appendix A). On the basis of their correlation for the local bed porosity, it is now possible to calculate an interstitial radial velocity profile using the relation $u/u_0 = (\varepsilon_b/\varepsilon)(v/v_0)$. This is also shown in Fig. 6. The radial interstitial velocity profile is less pronounced than the superficial velocity profile due to the compensating influence of the high porosity near the wall of the packed bed. In fact, Kirillov *et al.* (1979) and Caycik and Gunn (1988), who measured the local gas velocity inside a packed bed, found that the interstitial velocity does not significantly vary over the radius. But, if the local interstitial velocity is the same at every location on the radius, v_w will still be higher than v_c, because ε_w is higher than ε_c. The effective radial heat conductivity can now be calculated at every radial position, using the relation of

Table 2. Best fit values, goodness-of-fit and absolute mean error for the experiments with glass spheres in tube I with $D_t = 49.9$ mm

	One-region model				Two-region model			
Pe_p^l	$\lambda_{e,r}^*$	α_w^*	GOF	Error (%)	$\lambda_{e,r}^*$	α_w^*	GOF	Error (%)
268.9	16.69	20.05	4.7E − 2	7.0	13.64	19.88	1.4E − 5	11.4
392.9	21.87	23.24	1.3E − 1	7.0	17.85	22.97	1.5E − 5	11.4
522.4	25.16	31.70	2.5E − 1	5.4	19.52	34.09	1.8E − 5	9.4
691.0	31.79	36.31	1.9E − 1	4.7	24.84	39.55	7.4E − 7	7.6
852.7	40.93	36.10	7.1E − 1	5.3	33.36	37.11	1.1E − 3	8.6
991.0	44.47	39.31	9.3E − 1	3.0	35.57	40.91	1.2E − 2	5.9
1160.0	49.30	42.81	9.8E − 1	2.7	38.98	45.14	3.0E − 2	5.2
1313.6	54.42	44.74	1.0E0	2.3	43.49	46.85	2.6E − 1	4.6

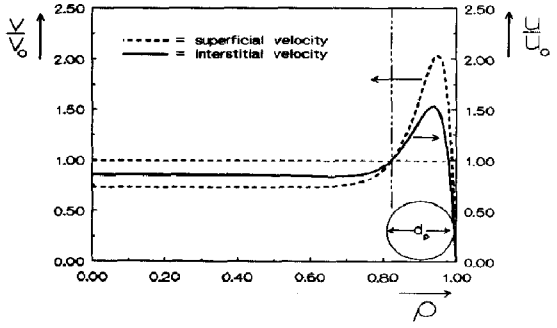

Fig. 6. Calculated radial superficial and interstitial velocity profiles for $N = 10$ and $Re_p^s = 500$.

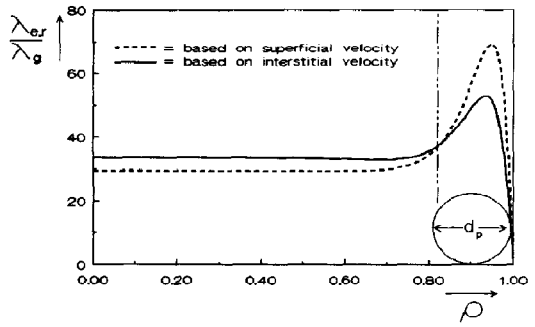

Fig. 7. Calculated effective radial heat conductivity profiles for $N = 10$ and $Re_p^s = 500$, using the velocity profiles from Fig. 6.

Zehner and Schlunder (1970, 1973) and using the two velocity profiles, respectively. This is shown in Fig. 7. On the basis of the superficial velocity, a reasonable difference is found between the effective heat conductivities in the core and the wall region. However, if the interstitial velocity is used, the difference is reduced significantly. Because, for high gas velocities, the rate of radial heat transport in packed beds is probably determined by the actual local velocity, we feel that the effective radial heat conductivity can be assumed

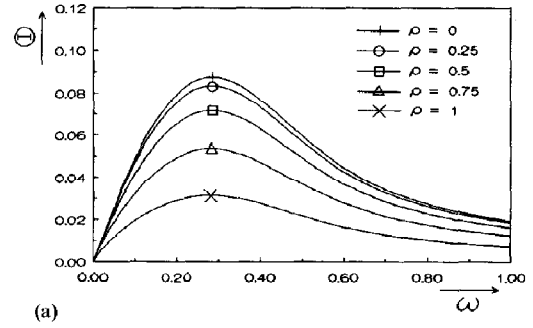

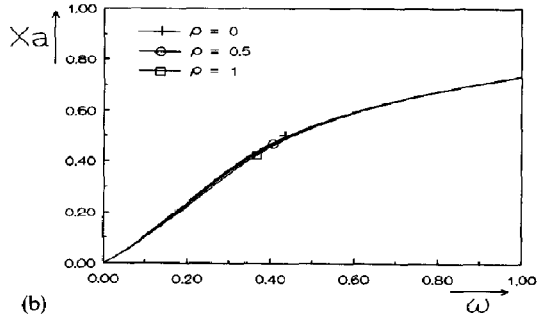

Fig. 8. Temperature and conversion profiles calculated with the one-region model for $N = 10$, $\Gamma = 100$ and $Re_p^s = 1000$, $\kappa = 15$, $Da_0 = 0.8$ and $\Delta T_{ad} = 0.6$. (A) Axial temperature profile, (B) axial conversion profile.

to be more-or-less independent of the radial superficial-velocity profile. Hennecke and Schlunder (1973) followed a similar line of reasoning and came to the same conclusion. So, the effective heat conductivities in the core region and wall region are assumed to be the same, or $\eta_h = 1$.

The wall effect with chemical reaction

In Fig. 8, calculated temperature and conversion profiles for the one-region model are given for selected values of the model parameters. The same profiles for the two-region model are given in Fig. 9, where the effective radial heat conductivity and the mass disper-

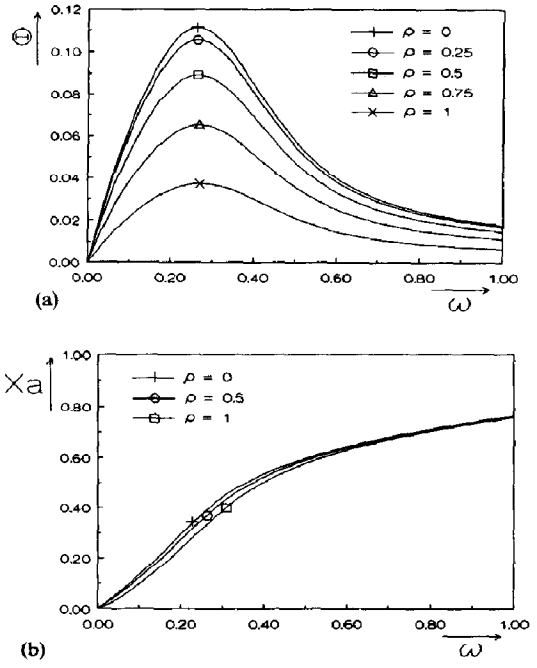

Fig. 9. Temperature and conversion profiles calculated with the two-region model for the same parameters as in Fig. 8 and with $\eta_h = \eta_m = 1$. (A) Axial temperature profile, (B) axial conversion profile.

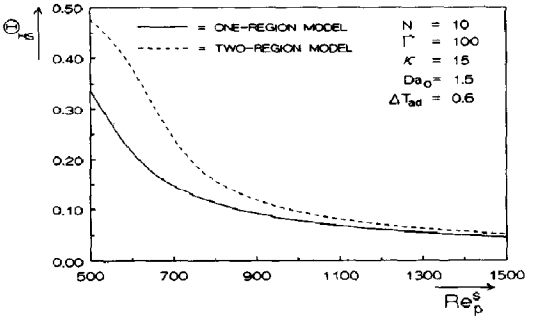

Fig. 10. Hot-spot temperatures for a fast first-order reaction with a moderate adiabatic temperature rise, with $\eta_h = \eta_m = 1$ and Da_0 based on $Re_p^s = 500$.

sion coefficient are taken constant over the radius. In Figs 10 and 11, the calculated hot-spot temperatures for the two models are given as a function of Re_p^s for constant values of the heat and mass transport coefficients over the radius. Figures 8–10 are calculated for a fast first-order reaction with a moderate heat effect and Fig. 11 is calculated for a slow first-order reaction with a large heat effect, like the oxidation of benzene to maleic anhydride [see Westerink and Westerterp (1988)] and the oxidation of ethylene [see Westerterp and Ptasinski (1984)], respectively.

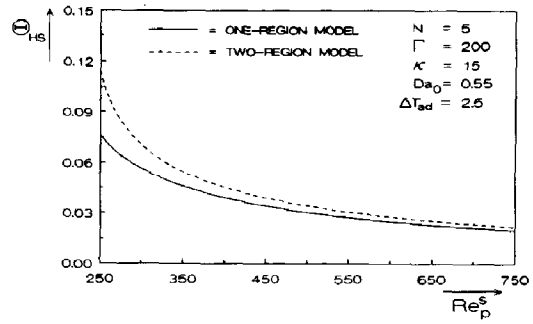

Fig. 11. Hot-spot temperatures for a slow first-order reaction with a large adiabatic temperature rise, with $\eta_h = \eta_m = 1$ and Da_0 based on $Re_p^s = 250$.

DISCUSSION AND CONCLUSIONS

Model calculations without a chemical reaction

We suggested that the effective radial heat conductivity in packed beds can be taken constant over the radius. Only the additional heat transfer resistance very close to the wall, which is found experimentally, might be incorporated in the effective heat conductivity by a sharp decrease of its value towards the wall. This is in principle equivalent to introducing a wall heat transfer coefficient, except at low Reynolds number [see Tsotsas and Schlunder (1990)]. Several arguments can be given for taking the effective radial heat conductivity as being constant over the radius:

—First, the influence of the velocity on the value of the effective heat conductivity, an increase of $\lambda_{e,r}$ with increasing v is opposed to the influence of the porosity profile, a decrease of $\lambda_{e,r}$ with increasing ε. Delmas and Froment (1988) give some functional relations between the local porosity, the velocity and the effective radial heat conductivity. But, the $\lambda_{e,r}$ profiles presented by them are not very pronounced over the radius of the bed due to the opposing effect of porosity and velocity. Only very close to the wall is a sharp decrease in the effective radial heat conductivity observed.

—Second, although the superficial radial velocity profile may be quite pronounced, the interstitial radial velocity profile is less so. If the rate of heat transport in a packed bed is determined by the local velocities, the values of the superficial velocities are not relevant.

—Third, the influence of the calculated temperature profiles of a difference in heat conductivity in the core and the wall region was found to be small, on the basis of literature relations.

—Fourth, there are only a few reports in literature on flattening of the experimentally determined radial temperature profile.

—Fifth, the experimental determination of local values for the effective heat conductivity is hardly possible, as a result of the fact that it is a bed scale parameter.

Recently, Daskowski and Eigenberger (1992) also concluded that the thermal radial conductivity may

be considered constant in radial and axial directions, provided a detailed flow model is used.

Taking the effective radial heat conductivity as being constant over the radius does not mean that a wall effect, if present, should not be taken into account when modelling heat transfer in a wall-cooled or wall-heated packed bed. Incorporation of the wall channelling of the gas will increase the predicted number of heat transfer units, due to the influence of the higher volumetric flow rate near the wall. For high Reynolds-particle numbers, of say higher than 500, and a low tube-to-particle diameter ratio, of say smaller than 20, the predicted differences are in the order of 10–20%, based on literature relations for the transport coefficients. For low values of the Reynolds-particle number, as for example used in apparatus for measuring kinetic data, this difference can even go up to 100% (see Fig. 2). This effect seems to be contradictory to the constancy of the interstitial velocity, but can be explained as follows. The porosity in the core is lower and in the wall region higher compared to the average bed porosity. As the interstitial velocity is constant, more than the average of the gas flow passes through the wall region and less than the average passes through the core. Because the distance to the wall is shorter, the gas flowing through the wall region is cooled more easily. The net effect of this higher flow through the wall region is that the total gas flow is cooled more easily than compared to the average flow rate; consequently, the NTU is higher than would be expected from calculations based on the average flow rate.

Model fitting without a chemical reaction

The differences between the measured and fitted profiles for the *one-region model* [see Fig. 3(b)] are randomly distributed over the bed, except at the tube wall. Often the differences between measured and fitted temperatures also increased towards the bed entrance. This is probably due to the fact that the temperature profile at the entrance of the packed bed is not constant over the radius as was assumed for the modelling. This, of course, has an influence on the values for the heat transport coefficients [see Borkink and Westerterp (1993)]. But, the influence of this entrance temperature profile is neglected here, because the one-region model is only qualitatively compared to the two-region model.

Correcting for the wall effect in the heat balance influences the values found for the heat transport coefficients (see Figs 4 and 5 and Table 2). For the *two-region model with two fit parameters*, being $\lambda_{e,r}$ and α_w, the effective radial heat conductivity is lowered about 20%, whereas the wall heat transfer coefficient hardly changes. This difference between the one-region model and the two-region model remains more-or-less constant for all velocities and for all three tubes. We estimated the difference in the number of heat transfer units to be about 15% for the conditions used in this study, when a wall effect is, or is not incorporated. This agrees well with the experimental results. We expected the differences between the one-region and the two-region model to decrease with an increasing number of particles on a diameter and increasing values of Pe_p^i. However, this is not observed. Probably the differences in the number of particles on a diameter —$N = 8$ for tube I to $N = 16$ for tube III—are not large enough and the values for Pe_p^i applied are already too high to notice a trend.

When the *two-region model with three fit parameters* $\lambda_{e,r}^c$, $\lambda_{e,r}^w$ and α_w is applied, unexpected values for the effective radial heat conductivity in the wall region are found, as can be seen from Fig. 5(a). The effective radial heat conductivity in the wall region is lowered, instead of being increased, whereas the wall heat transfer coefficient is increased. This can be explained by the fact that the measured averaged radial temperature profiles did not show any flattening whatsoever. Because of this, the model uses the extra degree of freedom for correcting for small errors in the measured temperatures close to the wall.

The GOF is low for low gas velocities (see Table 2). This can either be caused by an underestimation of the standard deviations for the measured temperatures, or the models are not suited for the description of the measured temperature profiles at low gas velocities. The temperature profile at the entrance was assumed to be flat, but, in practice, it might very well be parabolically shaped. This is expected to be more pronounced for low gas velocities, so the GOF is lowest in that case. From Table 2, it can also be seen that the GOF is always highest and the mean error lowest for the one-region model. This was nearly always found for all the measurements performed, including those which were performed with alumina cylinders and Raschig rings. This result may be caused by either the non-existence of the phenomenon of wall channelling or by an erroneous description of it. If there is no such thing as a higher superficial velocity at the wall and nevertheless it is incorporated in the model, this necessarily must lead to a lower GOF. Some authors [see, e.g., Kirillov *et al.* (1979) and Caycik and Gunn (1988)] found that the radial interstitial velocity is constant over the radius. It would require further research to make sure whether there is a pronounced superficial velocity profile present inside the packed bed and, if so, how it should be incorporated in the heat balances for a wall-cooled or wall-heated packed bed and the cooled tubular reactor.

From the preceding, it has become clear that, especially at low values for Re_p^s, say < 100, and a small number of particles on a diameter, say < 20, the differences between the values for the heat transport coefficients obtained from a model with and without a wall effect can be very high, up to 50%. For higher values of the Reynolds number, the differences decrease to about 20%.

It should be noted that, if a radial velocity profile is taken into account when heat transport parameters are obtained from cold-flow experiments, it must also be used to calculate the heat and mass transport in

a cooled tubular reactor with reaction. Otherwise, the influence of the radial velocity profile is only lumped into the heat transport parameters and the reactor calculations will yield erroneous results.

Model calculations with a chemical reaction

The incorporation of a porosity and velocity profile in the heat and mass balances results in a significant change in the predicted temperature profiles for a cooled tubular reactor. The wall effect changes the value of the calculated hot-spot temperature, as was also found by Lerou and Froment (1977), Kalthoff and Vortmeyer (1980), McGreavy *et al.* (1986), Gatica *et al.* (1989) and Vortmeyer and Haidegger (1991). This is partly due to the lower superficial gas velocity in the centre of the bed, but the effect of the higher amount of catalyst—and therefore reaction rate per unit of volume—present in the core-region, because of the lower porosity, is much more pronounced. The differences in calculated hot-spot temperatures for the one-region and two-region model can be as high as 80%, if compared to the coolant temperature. For conditions which correspond to practice, the differences in calculated hot-spot temperatures are in the order of 15–20%. These figures were calculated based on literature relations for the heat and mass transport coefficients and assuming these to be constant over the radius. If the effective radial heat conductivity is not taken constant over the radius, slightly larger differences are found. If the reactor is even more close to runaway—a situation often looked at in literature—the differences are still larger. But, it should be noted that, in that case, every minor change in one of the model parameters has a great impact on the results.

So, for the modelling of cooled tubular reactors, the inclusion of a wall effect, especially the radial porosity profile, may be very important. But, more research is needed to determine whether there is a significant change in superficial velocity over the radius in, and not only above, the packed bed, and, if so, how to incorporate this in the heat and mass balances. If it is present, it should be taken into account, but the effective radial heat conductivity can be assumed to be constant over the radius.

NOTATION

A_p external surface area of a particle, m^2

Bi_t tube Biot number ($= \alpha_w R_t/\lambda_{e,r}$), dimensionless

$Bo_{h,r}$ radial Bodenstein number for heat, ($= \rho_g Cp_g v d_p/\lambda_{e,r}$), dimensionless

$Bo^{\ominus}_{h,r}$ modified radial Bodenstein number for heat ($= \rho_g Cp_g v R_t^2/\lambda_{e,r} L$) $= (Bo_{h,r} N/4\Gamma)$, dimensionless

$Bo_{m,r}$ radial Bodenstein number for mass ($= v d_p/D_{e,r}$), dimensionless

$Bo^{\ominus}_{m,r}$ modified radial Bodenstein number for mass ($= v R_t^2/D_{e,r} L$) $= (Bo_{m,r} N/4\Gamma)$, dimensionless

C_A concentration of component A, mole m^{-3}

Cp_g heat capacity at constant pressure for the gas, $J\,kg^{-1}\,K^{-1}$

d_p particle diameter, m

d_p^e equivalent diameter of a sphere ($= 6V_p/A_p$), m

Da_0 Damkohler number based on the empty tube [$= Lk_0 \exp(-\kappa)/v_0$], dimensionless

$Da^{\ominus}$ modified Damkohler number $\{= (1-\varepsilon)/(1-\varepsilon_b)[Lk_0 \exp(-\kappa)/v] = (Da_0/v)(1-\varepsilon)/(1-\varepsilon_b)\}$, dimensionless

$D_{e,r}$ effective radial mass disperison coefficient, $m^2\,s^{-1}$

D_t tube diameter, m

E activation energy, $J\,mol^{-1}$

G superficial gas mass flow rate, $kg\,m^{-2}\,s^{-1}$

ΔH_r reaction enthalpy, $J\,mol^{-1}$

J_0, J_1 zeroth-order and first-order Bessel functions of the first kind [see Abramowitz and Stegun (1972)]

k_0 pre-exponential factor, s^{-1}

L bed length, m

N number of particles on a diameter ($= D_t/d_p$), dimensionless

NTU number of heat transfer units, dimensionless

Pe_p^i Peclet number, based on the interstitial velocity ($= \rho_g Cp_g u d_p^e/\lambda_g = Re_p^i Pr$), dimensionless

Pr Prandtl number for the gas ($= \eta_g Cp_g/\lambda_g$), dimensionless

$P_0(a,b)$ $= J_0(a)Y_0(b) - J_0(b)Y_0(a)$

$P_1(a,b)$ $= J_1(a)Y_1(b) - J_1(b)Y_1(a)$

$Q_0(a,b)$ $- J_0(a)\,\partial Y_0(b)/\partial b - Y_0(a)\,\partial J_0(b)/\partial b$

r radial coordinate, m

R gas constant, $J\,mol^{-1}\,K^{-1}$

R_c radius of the core region, m

R_t tube radius, m

Re_p^i Reynolds number, based on the interstitial velocity ($= \rho_g u d_p^e/\eta_g$), dimensionless

Re_p^s Reynolds-particle number based on the superficial velocity ($= \rho_g v d_p/\eta_g$), dimensionless

T temperature, K

ΔT_{ad} dimensionless adiabatic temperature rise ($= |\Delta H_r| C_A^{in}/\rho_g Cp_g T_{ct}$), dimensionless

u interstitial gas velocity ($= v/\varepsilon$), $m\,s^{-1}$

v superficial gas velocity, $m\,s^{-1}$

V_p volume of a particle, m^3

X conversion of component A [$= (C_A^{in} - C_A)/C_A^{in}$], dimensionless

Y_0, Y_1 zeroth-order and first-order Bessel functions of the second kind [see Abramowitz and Stegun (1972)]

z axial coordinate, m

Greek letters

α_w	wall heat transfer coefficient, W $m^{-2} K^{-1}$
α_w^*	dimensionless wall heat transfer coefficient ($= \alpha_w d_p^e/\lambda_g$), dimensionless
γ	dimensionless width of the core region ($= R_c/R_t$), dimensionless
Γ	tube slenderness ($= L/D_t$), dimensionless
ε	porosity, dimensionless
ε_b	average porosity of the bed, dimensionless
η_g	dynamic viscosity of the gas, Pa s
η_h	quotient of the effective heat conductivities ($= \lambda_{e,r}^c/\lambda_{e,r}^w$), dimensionless
η_m	quotient of the effective mass dispersion coefficients ($= D_{e,r}^c/D_{e,r}^w$), dimensionless
θ	dimensionless temperature for the case without reaction [$= (T - T_{cl})/(T_{in} - T_{cl})$], dimensionless
Θ	dimensionless temperature for the case with reaction [$= (T - T_{cl})/T_{cl}$], dimensionless
κ	dimensionless activation energy ($= E/RT_c$), dimensionless
$\lambda_{e,r}$	effective radial heat conductivity, W $m^{-1} K^{-1}$
λ_g	heat conductivity of the gas, W $m^{-1} K^{-1}$
λ_r^*	dimensionless effective radial heat conductivity ($= \lambda_{e,r}/\lambda_g$), dimensionless
μ	$= \sqrt{(Bo_{h,r}^{c\Theta}/Bo_{h,r}^{w\Theta})}$
v	dimensionless superficial velocity ($= v/v_0$), dimensionless
ν_p	stoichiometric coefficient, dimensionless
ρ	dimensionless radial coordinate ($= r/R_t$), dimensionless
ρ_g	density of the gas kg m^{-3}
σ	standard deviation, dimensionless
χ^2	chi-square target function
ω	dimensionless axial coordinate ($= z/L$), dimensionless

Subscripts

0	empty tube
c	core region
cl	coolant
e	effective
in	inlet conditions
p	particle
s	solid
t	tube
w	wall region or wall

Superscripts

c	core region
e	equivalent
i	interstitial
s	superficial
w	wall region

REFERENCES

Abramowitz, M. and Stegun, I. A., 1972, *Handbook of Mathematical Functions, with Formulas, Graphs and Mathematical Tables*. Wiley, New York.

Agnew, J. B. and Potter, O. E., 1970, Heat transfer properties of packed tubes of small diameter. *Trans. Instn chem. Engrs* **48**, T15–T20.

Borkink, J. G. H., 1991, Heat transport in wall-cooled packed beds of low tube-to-particle diameter ratio. Thesis, Twente University of Technology, Quick Service, Enschede, The Netherlands.

Borkink, J. G. H. and Westerterp, K. R., 1992, Influence of tube and particle diameter on heat transport in packed beds. *A.I.Ch.E. J.* **38**, 703–715.

Borkink, J. G. H., Borman, P. C. and Westerterp, K. R., 1993, Modeling of radial heat transport in packed beds—confidence intervals of estimated parameters and choice of boundary conditions. *Chem. Engng Commun.* **121**, 135–155.

Bos, A. N. R. and Westerterp, K. R., 1991, The mass balance for gas phase reactions in tubular reactors. *Chem. Engng Commun.* **99**, 139–153.

Botterill, J. S. M. and Denloye, A. O. O., 1978, A theoretical model of heat transfer to a packed or quiescent fluidized bed. *Chem. Engng Sci.* **33**, 509–515.

Caycik, M. and Gunn, D. J., 1988, True mean velocities in the wall and bulk regions of fixed beds. *Chem. Engng Sci.* **43**, 1637–1646.

Cheng, P. and Vortmeyer, D., 1988, Transverse thermal dispersion and wall channeling in a packed bed with forced convective flow. *Chem. Engng Sci.* **43**, 2523–2532.

Daskowski, T. and Eigenberger, G., 1992, A re-evaluation of fluid flow, heat transfer and chemical reaction in catalyst filled tubes. *Chem. Engng Sci.* **47**, 2245–2250.

Delmas, H. and Froment, G. F., 1988, A simulation model accounting for structural radial nonuniformities in fixed bed reactors. *Chem. Engng Sci.* **43**, 2281–2287.

De Wasch, A. P. and Froment, G. F., 1972, Heat transfer in packed beds. *Chem. Engng Sci.* **27**, 567–576.

Dixon, A. G., 1988, Wall and particle-shape effects on heat transfer in packed beds. *Chem. Engng Commun.* **71**, 217–237.

Eigenberger, G. and Ruppel, W., 1985, Problems der Modellbildung bei technischen Festbettreaktoren. *Chem. Engng Technol.* **57**, 181–190.

Fahien, R. W. and Smith, J. M., 1955, Mass transfer in packed beds. *A.I.Ch.E. J.* **1**, 28–37.

Feyo de Azevedo, S., Romero-Ogawa, M. A. and Wardle, A. P., 1990, Modelling of tubular fixed-bed catalytic reactors: a brief review. *Trans. Instn chem. Engrs* **68**, 483–502.

Freiwald, M. G. and Paterson, W. R., 1992, Accuracy of model predictions and reliability of experimental data for heat transfer in packed beds. *Chem. Engng Sci.* **47**, 1545–1560.

Gatica, J. E., Romagnoli, J. A., Errazu, A. F. and Porras, J. A., 1989, Steady and non-steady state modeling of tubular fixed bed reactors. *Chem. Engng Commun.* **78**, 73–96.

Gunn, D. J., Ahmad, M. M. and Sabri, M. N., 1987, Radial heat transfer to fixed beds of particles. *Chem. Engng Sci.* **42**, 2163–2171.

Haidegger, E., Vortmeyer, D. and Wagner, P., 1989, Simultane Lösung von Energie-, Stoff- and Impulsgleichungen für wandgekühlte chemische Festbettreaktoren. *Chem. Engng Technol.* **61**, 647–650.

Hennecke, F. W. and Schlünder, E. U., 1973, Wärmeübergang in beheizten oder gekühlten Rohren mit Schüttungen aus Kugeln, Zylindern und Raschig-Ringen. *Chem. Engng Technol.* **45**, 277–284.

Kalthoff, O. and Vortmeyer, D., 1980, Ignition/extinction phenomena in a wall cooled fixed bed reactor: experiments and model calculations including radial porosity and velocity distributions. *Chem. Engng Sci.* **35**, 1637–1643.

Kirillov, V. A., Kuz'min, V. A., P'yanov, V. I. and Khanaev, V. M., 1979, Velocity profile in a stationary granular bed. Translated from *Doklady Akademii Nauk SSSR* **245**, 159–162.

Lerou, J. J. and Froment, G. F., 1977, Velocity, temperature and conversion profiles in fixed bed catalytic reactors. *Chem. Engng Sci.* **32**, 853–861.

Li, C. H. and Finlayson, B. A., 1977, Heat transfer in packed beds—a re-evaluation. *Chem. Engng Sci.* **32**, 1055–1066.

McGreavy, C. and Foumeny, E. A., 1986, Prediction of transport parameters for fixed bed reactors. *Trans. World Congr.* III *Chem. Engng*, Tokyo, pp. 342–345.

McGreavy, C., Foumeny, E. A. and Javed, K. H., 1986, Characterization of transport properties for fixed bed in terms of local bed structure and flow distribution. *Chem. Engng Sci.* **41**, 787–797.

Olbrich, W. E. and Potter, O. E., 1972, Heat transfer in small diameter packed beds. *Chem. Engng Sci.* **27**, 1723–1732.

Paterson, W. R. and Carberry, J. J., 1983, Fixed bed catalytic reactor modelling: the heat transfer problem. *Chem. Engng Sci.* **38**, 175–180.

Press, W. H., Flannery, B. P., Teukolsky, S. A. and Vetterling, W. T., 1989, *Numerical Recipes in Pascal: the Art of Scientific Computing*. Cambridge University Press, Cambridge.

Tsotsas, E. and Schlünder, E. U., 1988, Some remarks on channeling and on radial dispersion in packed beds. *Chem. Engng Sci.* **43**, 1200–1203.

Tsotsas, E. and Schlünder, E. U., 1990, Heat transfer in packed beds with fluid flow: remarks on the meaning and the calculation of a heat transfer coefficient at the wall. *Chem. Engng Sci.* **45**, 819–837.

Villadsen, J. V. and Stewart, W. E., 1967, Solution of boundary-value problems by orthogonal collocation. *Chem. Engng Sci.* **22**, 1483–1501.

Vortmeyer, D. and Schuster, J., 1983, Evaluation of steady flow profiles in rectangular and circular packed beds by a variational method. *Chem. Engng Sci.* **38**, 1691–1699.

Vortmeyer, D., 1988, Packed bed models and convective flow. *Proceedings* 1988 *Nat. Heat Transf. Conference* HDT-Vol. 96, Vol. 1, pp. 755–766.

Vortmeyer, D. and Haidegger, E., 1991, Discrimination of three approaches for wall-cooled fixed bed reactors. *Chem. Engng Sci.* **46**, 2651–2660.

Wellauer, T., Cresswell, D. L. and Newson, E. J., 1982, Heat transfer in packed reactor tubes suitable for selective oxidation. *ACS Symp. Ser.* **169**, 527–542.

Westerterp, K. R. and Ptasinski, K. J., 1984, Safe design of cooled tubular reactors for exothermic, multiple, reactions; parallel reactions—II. *Chem. Engng Sci.* **39**, 245–252.

Westerink, E. J. and Westerterp, K. R., 1988, Safe design of cooled tubular reactors for exothermic multiple reactions: multiple reaction networks. *Chem. Engng Sci.* **43**, 1051–1069.

Wijngaarden, R. J., 1988, The scaling-up of cooled tubular reactors. Thesis, Twente University of Technology, Burgo druk, Goor.

Zehner, P. and Schlünder, E. U., 1970, Wärmeleitfähigkeit von Schüttungen bei mäszigen Temperaturen. *Chem. Engng Technol.* **42**, 933–941.

Zehner, P. and Schlünder, E. U., 1973, Die effective Wärmeleitfähigkeit durchströmter Kugelschüttungen bei mäszigen und hohen Temperaturen. *Chem. Engng Technol.* **45**, 272–276.

Ziolkowski, D. and Legawiec, B., 1987, Remarks upon thermokinetic parameters of the one- and two-dimensional mathematical models of heat transfer in a tubular flow apparatus with a packed bed. *Chem. Engng Process.* **21**, 65–76.

APPENDIX A: RADIAL POROSITY AND VELOCITY PROFILES

The mathematical description proposed by Vortmeyer and Schuster (1983) for the radial porosity profile in a tubular packed bed filled with spherical particles is given by

$$\varepsilon = \varepsilon_\infty \{1 + K \exp[-N(1-\rho)]\}. \quad \text{(A1)}$$

The constants in eq. (A1) used by Vortmeyer and Schuster (1983) are $\varepsilon_\infty = 0.4$ and $K = 1$, respectively, so that the porosity at the wall is 0.8 [see also Cheng and Vortmeyer (1988) and Haidegger *et al.* (1989)]. In Fig. 1(a), this profile is shown. For the calculation of the radial superficial velocity profile, the following equation is proposed by them:

$$v = C\{1 - [1 - A(1-\rho)] \exp[B(1-\rho)]\} \quad \text{(A2)}$$

in which

$$A = \begin{cases} 0.5N[-1803 + 201.62(\ln Re_p^s + 4) - 3737(\ln Re_p^s + 4)^{1/2} + 5399(\ln Re_p^s + 4)^{1/3}] & \text{for } 1 \leqslant Re_p^s \leqslant 1000 \\ 13.5N \quad \text{for } Re_p^s > 1000 \end{cases} \quad \text{(A3)}$$

$$B = \frac{2NA}{(2N - A)} \quad \text{(A4)}$$

$$C = \frac{1}{\left[1 + (1+B)(1-A)\frac{2}{B^2} + \frac{A}{B}\left(2 + \frac{4}{B} + \frac{4}{B^2}\right) - \frac{2}{B^2}\left(1 - A + \frac{2A}{B}\right)\exp(B)\right]}. \quad \text{(A5)}$$

The expression for the constant C, given in the original paper, contains some typographical mistakes [see also Tsotsas and Schlunder (1988)]. With these equations it is possible to calculate the profile shown in Fig. 1(b).

APPENDIX B: STEP FUNCTIONS FOR THE POROSITY AND VELOCITY PROFILES

The width of the core region γ is taken as the smallest radius ending at the radial point where $v = 1$. This yields

$$C[1 - \{1 - A(1-\gamma)\} \exp\{B(1-\gamma)\}] = 1 \quad \text{(B1)}$$

from which γ can be found by trial-and-error. The porosities in the core region and wall region are found according to

$$\varepsilon_c = \frac{2}{\gamma^2}\int_0^\gamma \varepsilon(\rho)\rho\,\partial\rho \quad \text{and} \quad \varepsilon_w = \frac{2}{1-\gamma^2}\int_\gamma^1 \varepsilon(\rho)\rho\,\partial\rho. \quad \text{(B2)}$$

The integrals in these equations are given by

$$\int_-^- \varepsilon(\rho)\rho\,\partial\rho = \left\{0.2\rho^2 + 0.4\frac{(N\rho - 1)}{N^2}\exp[-N(1-\rho)]\right\}\Bigg|_-^- \quad \text{(B3)}$$

provided $\varepsilon(\rho)$ is given by eq. (A1). The average velocities in the core region and wall region are found according to

$$v_c = \frac{2}{\gamma^2}\int_0^\gamma v(\rho)\rho\,\partial\rho \quad \text{and} \quad v_w = \frac{2}{1-\gamma^2}\int_\gamma^1 v(\rho)\rho\,\partial\rho. \quad \text{(B4)}$$

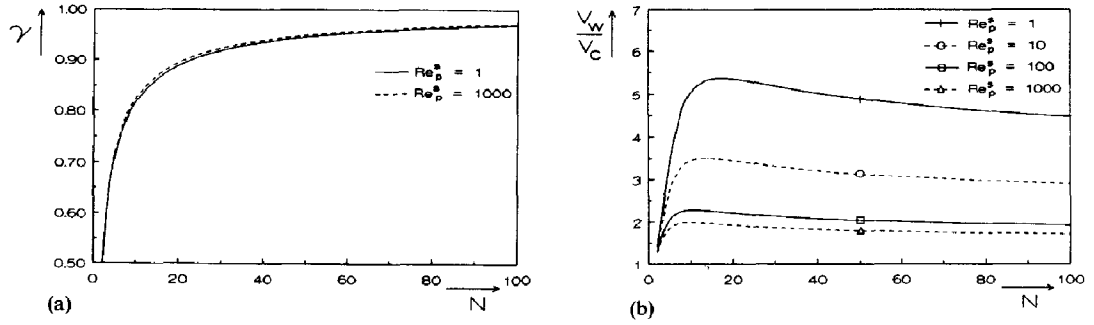

Fig. A1. Calculated values for γ and v_w/v_c as a function of N and for different Re_p^s. (A) Width of the core region, (B) ratio of the velocities.

The integrals in these equations are given by

$$\int_{-}^{-} v(\rho)\rho\,\partial\rho = C\left[0.5\rho^2 + \frac{(1+B\rho)}{B^2}\left[1+\frac{A}{B}-A(1-\rho)\right] \times \exp\left[B(1-\rho)\right] + \frac{A}{B^2}\exp\left[B(1-\rho)\right]\right]\Bigg|_{-}^{-} \quad \text{(B5)}$$

provided $v(\rho)$ is given by eq. (A2). In Fig. A1, calculated values for γ and for $v_w/v_c = v_w/v_c$ are given.

The width of the core-region is a function of the number of particles on a diameter N and independent of the Reynolds number. The width of the wall region varies from 0.75 to 1.25 times the particle diameter for the range N = 5–100. For high values of N, of say higher than 20, the ratio of the velocities becomes almost constant. Also for high values of the Re_p^s number, say 100, the ratio becomes almost constant. There is a maximum in the ratio in the region between 5 and 15 particles on a diameter. For a large number of particles on a diameter, the influence of a wall effect on the heat transport in cooled tubes vanishes due to a small value of the volume fraction taken up by the wall region; for a small number of particles on a diameter also, it vanishes because the value of v_w/v_c approaches unity.